

Multi-scale quantitative risk analysis of seabed minerals: principles and application to seafloor massive sulfide prospects

Cyril Juliani, Steinar Løve Ellefmo

Norwegian University of Science and Technology (NTNU), Department of Geoscience and Petroleum, Sem
Sælandsvei 1, 7491, Trondheim, Norway

Corresponding author: Cyril Juliani

Corresponding e-mails: cyril.juliani@ntnu.no, steinar.ellefmo@ntnu.no

Phone number: +47 93 07 85 44

ORCID: orcid.org/0000-0001-8613-8382

Keywords play analysis, prospect, deep-sea minerals, resource management, risk, seafloor massive sulfide

Acknowledgements

Very helpful corrections and comments by Stephen John Lippard and Richard Sinding-Larsen improved the quality of this paper. Two anonymous reviewers also improved many aspects of the early manuscript draft with important suggestions. This work was made possible with bathymetric data acquired during the MarMine cruise by the Norwegian University of Science and Technology (NTNU).

Abstract

The potential for mining hydrothermal mineral deposits on the seafloor, such as seafloor massive sulfides (SMS), has become technically possible and some companies (currently not many) are considering their exploration and development. Yet, no present methodology has been designed to quantify the ore potential and assess the risks relative to prospectivity at prospect and regional scales. Multi-scale exploration techniques, similar to those of the play analysis that are used in the oil and gas industry, can help to fulfill this task by identifying the characteristics of geologic environments indicative of ore-forming processes. Such characteristics can represent a combination of e.g.,

heat source, pathway, trap and reservoir that all dictate how and where ore components are mobilized from source to deposition. In this study, the understanding of these key elements is developed as a mineral system, which serves as a guide for mapping the risk of the presence or absence of ore-forming processes within the region of interest (the permissive tract). The risk analysis is carried out using geoscience data, and it is paired with quantitative resource estimation analysis to estimate the in-place mineral potential. Resource estimates are simulated stochastically with the help of available data (bathymetric features in this study), conventional grade-tonnage models and Monte-Carlo simulation techniques. In this paper, the workflow for a multi-scale quantitative risk analysis, from the definition to the evaluation of a permissive tract and related prospect(s), is described with the help of multi-beam data of a known hydrothermal vent site.

1. Introduction

The discovery of hydrothermal vent fields along mid-ocean ridges (MORs) (Beaulieu et al. 2013) has led to the emergence of ocean exploration and development companies who are working to exploit deeply seated minerals (Miller et al. 2018) such as seafloor massive sulfides (SMS). Such interests have led to exploring deep ocean floors (most SMS deposits are within 2 to 3 km-depth range; Hannington et al. 2010) and poorly understood marine environments (20% of MORs investigated; Baker and German 2004). At present, known SMS provide important clues about their likely distribution, size and grade (Hannington et al. 2010, 2011), but the lack of direct information from drilling, which is crucial to estimate the characteristics of undiscovered mineral deposits (e.g., grade and tonnage), does not permit the realization of proper assessments of these resources. Yet, the exploration for seabed minerals may become, just as for petroleum exploration activities (billions of US dollars yearly; e.g., Norwegian Petroleum Directorate 2017), a business that requires significant investment for diverse offshore operations including expensive exploration drilling. Mineral exploration, by definition, necessarily involves risk, i.e. the chance of project failure or financial loss, that can be addressed within a geological, technical and economic context (e.g., Otis and Schneidermann 1997; Jones and Hillis 2003; Schiozer et al. 2004; Suslick et al. 2009). This paper focuses on the definition and the management of these risks. From a geologic perspective, the risk originates from the possibility that e.g., resource evaluations do not accurately estimate what is actually present or the resource sought does not exist in the region of interest. In onshore mineral exploration, these concerns can be better understood with the help of assessment methodologies, such as the three-part assessment form (Singer and Menzie 2010), which undertakes

quantitative and qualitative evaluation of mineral resources (i.e., number of undiscovered deposits and related grade and tonnage variations) based upon conventional deposit models (e.g., [Cox and Singer 1986](#)). The deposit model is a concept of what is significant in terms of ore occurrence in geological, geophysical and, or, geochemical data.

However, as data may be of variable quality or simply missing, information about metal-bearing minerals possibly concealed beneath the seafloor can be unclear and lead to failed assessments. In such circumstances, the prospect risk is amplified, and it is thus necessary for a preliminary explorative study to engage efforts in evaluating and reducing these risks within areas identified to likely contain potential ore accumulations.

Up to now, multi-scale exploration techniques, such as the play analysis methods for petroleum exploration (see [White, 1988, 1993](#)), have helped to advance the analysis and interpretation of data and build crucial information that mitigate the risk of exploration (e.g., [Gautier et al. 1995](#); [Dutton et al. 2003](#); [Attanasi and Freeman 2009](#)). The play-based approach aims at evaluating the prospectivity of groups of oil fields based on geological processes, such as trap formation and oil generation, migration and accumulation ([Allen and Allen 2013](#)). Combined, these processes adjust the resource prospectivity within a delineated region where favorable grounds can be separated into a mosaic of risked areas ([Grant et al. 1996](#)). In mineral exploration, we can delineate this region where the geology is permissive for the existence of deposits of one or more types, i.e. the permissive tract ([Singer 1993](#)), and where numbers of potential mineral deposits (prospects) may occur. For preliminary exploration of both the permissive tracts and prospects, a conceptual targeting strategy can be developed by using the mineral system concept ([Wyborn et al. 1994](#)), which uses analogous principles to investigate the mobilization, accumulation and preservation of ore components within the mineral system of interest. These principles serve as a basis to find where to look for undiscovered ore accumulations and to determine the risks related to exploration. In the context of seabed mineral exploration, a risk analysis can be made by using all available seafloor data (e.g., video, multi-beam and geophysical data; [Lipton 2012](#)) which, combined with the assessment of the potential endowment of a deposit within the mineral system, drives decisions related to pursuing exploration activities. The exploration risk depends on the probability that certain geological factors of the mineral system (i.e., heat source, pathway, reservoir and trap) represent adequate conditions for triggering ore genesis. The attribution of probabilities to the adequacy of such factors derives from the interpretation of geoscience data. The metal endowment quantification, on the other hand, can be processed in multiple ways, either with the help of pre-established grade-tonnage models (e.g., [Singer 2008](#); [Mosier et al. 2009](#))

and, or, directly from drilling (e.g., [Hannington et al. 1998](#)) and high-resolution bathymetry (e.g., [Jamieson et al. 2014](#)). The most likely abundances of ore metals can be calculated stochastically using conventional Monte-Carlo techniques and expressed in the form of probability distributions that capture the full range of uncertainty in the evaluated resource occurrence at different prediction levels (e.g., 10th, 50th and 90th percentiles).

In this paper, an example of multi-scale quantitative risk analysis for SMS deposits will be applied to the Loki's Castle vent field area (73°34'N; [Pedersen et al. 2010](#)) located at the northern part of the Mohns Ridge (71-73°N). The aim of this paper is to use mineral system, permissive tract-prospect hierarchy and related risk mapping concepts, and the quantification of risk and ore volumes, to identify and evaluate geologic environments favorable for ore genesis within the study area.

2. Multi-scale exploration: permissive tract, camp and prospect

2.1. Definitions and overview

Play-based exploration (see [White, 1988, 1993](#)) is the basis and inspiration for developing quantitative evaluation methods of seabed minerals in this study. It is intended to build and leverage the understanding of a geological system in which a range of exploration activities might be conducted for undiscovered resources (e.g., [Gautier et al. 1995](#); [Dutton et al. 2003](#); [Attanasi and Freeman 2009](#)). In its application, geological factors, that are critical for the generation of natural resources are documented and mapped in exploration areas. In the context of SMS genesis, factors can include host rocks in which metals accumulate or regional heat sources driving the circulation of metal-rich fluids within the oceanic crust. These factors can be described in the form of a mineral system (see section 2.2; [Hronsky and Groves 2008](#); [McCuaig and Hronsky 2014](#); [Hagemann et al. 2016](#)) where multi-scale geological processes and corresponding footprints are described and mapped to provide a source-transport-trap analysis that can be used to assess undiscovered mineral deposits ([Hagemann et al. 2016](#)). The mapped geological evidence allows the delineation of the most prospective regions (permissive tracts; [Singer, 1993](#)), which are then used to map mineral exploration targets at a regional scale (e.g., among the neo-volcanic zones of a MOR; [Juliani and Ellefmo, 2018](#)).

As conceived by [Singer \(1993\)](#) for prospecting mineral deposits, a permissive tract represents extended frontiers of terrains for which geologic environments permit a deposit type to form. Beyond those frontiers, the probability of

occurrence for new findings is negligible for the deposit type considered. Inside a tract, however, potential mineral deposits (prospects) can be individually assessed on the basis of early geophysical, geological and, or, geochemical survey results. Neighboring prospects can be grouped into a “camp”. A camp may include one or more mineral prospects representing a single deposit type, and it shares common geological factors for the presence of potential mineral resources with other camps in a specific permissive tract. The delineation of a camp derives from the decisions made by prospectors about the way prospects are grouped for the resource assessment, while permissive tract and prospects represent geological subdivisions. For that matter, it will be up to prospectors to decide (1) a maximum distance between prospects considered for clustering, and (2) whether or not to group prospects that are genetically and, or temporally unrelated, i.e. prospects in close proximity that are not necessarily coeval nor controlled by the same seafloor structure such as a fault. The objectives of this hierarchical analysis are (1) to narrow down areas with specific combinations of geological factors controlling undiscovered resources in a region, and (2) to make geologically proper assessments of these resources in the areas of interest. Furthermore, this multi-scale analysis would facilitate offshore mineral exploration by cataloguing exploration projects (permissive tracts and camps) and associated mineral occurrences (prospects). Up to now, SMS deposits investigated at MORs are essentially inferred at seafloor, even though some buried deposits may be studied, just like oil and gas volumes, at depth intervals below the seafloor. A simplified organizing scheme of the permissive tract-camp-prospect concept is presented on Fig.1 given that target areas are thought to contain mineral deposits at seafloor and not deep in the crust. Sophisticated technology may help to detect and determine the extent of these deposits and, or, features of the sub-surface geology using exploration geophysics. The surveyed areas that are prospective for ore minerals may be distinguished into camps and prospects. Both target features can be given priority e.g., for drilling given the inferences made on their mineral potential, or for mining given the type of resource evaluated and the mining system applied by the investigating company.

2.2. Mineral system

The mineral system concept is used, just as the play analysis, to interrogate the unknown and, in addition, it presents known information on the genesis of ore within wide-scaled geological processes ([Hronsky and Groves 2008](#); [McCuaig and Hronsky 2014](#); [Hagemann et al. 2016](#)). Studying a mineral system helps geoscientists understand (1) the nature of the ore-forming processes being responsible for the formation of metal accumulation(s) within a limited

spatial and time frame, and (2) the genetic relation existing between the produced ore and the critical processes operating within a region that may be considered for a multi-scale analysis. Key elements of the system are commonly defined as source of fluids and metals, heat source(s), migration pathway, trap and outflow zone (Wyborn et al. 1994; Knox-Robinson and Wyborn 1997). By adopting this concept, an exploration geologist can interrogate available data and map geological features associated with migration, entrapment and the genesis of metals. For the purpose of this study, we propose a mineral system that is assumed to correspond to mineralization processes active within the axial neo-volcanic terrains of the Mohns Ridge (Table 1):

- (1) **Heat source:** the energy driving hydrothermal cells during seafloor spreading, i.e. the heat from an underlying magma source.
- (2) **Pathways:** crustal heterogeneities, such as faults and fractures, providing fluid migration paths for hydrothermal circulation and focused outflows (McCaig et al. 2007).
- (3) **Trap:** physical and, or, chemical reaction mechanisms (e.g., low-permeability barriers, fluid mixing and redox reactions) leading to in-situ metal precipitations.
- (4) **Reservoir:** the discharge of a hydrothermal system, where precipitated metals are preserved from oxidizing conditions and dissolution. The reservoir rock can be constructional (e.g., the massive sulfide mound itself) and, or, be from the hydrothermal replacement of the host rock by sulfide mineralization and alteration products (e.g., the mineralized stockwork). Both, the reservoir rock and the trap can provide required structural architecture for depositional and sealing mechanisms that limit the dispersion and dilution of hydrothermal fluids.

Because the underlying geology (heat source and pathway), combined with the depositional environment (reservoir and trap), generally demonstrates diverse and complex sets of multi-scale processes, evaluating the resource potential of an area will depend, among others, on the scale of the study area. Smaller scale study areas will comprise finer details and make the understanding of a permissive tract (province-scale) geologically more accurate if data acquisition is carried out at the camp-prospect levels (district to deposit scale, as described by Hronsky and Groves 2008). The current understanding of the trap mechanism for SMS is generally limited to small-scale processes, such as the transport, entrainment and deposition of sedimentary debris (Clague and Stead, 2012), which offer better potential for mineralization preservation (e.g., Koski et al. 1994). Similarly, conductive cooling and hydrothermal fluids mixing with seawater can induce in-situ thermodynamic trapping (e.g., at the TAG vent field; Tivey et al.,

1995,1998; Mills et al., 1998; Mills and Tivey, 1999). Although ambient seawater can be considered as an extensive controlling factor for mineralization, it does not critically help refining the permissive tract evaluation. In comparison, the heat source can be mapped from major features below or at the seafloor, as shown by e.g., the extended geophysical signature of axial magma chamber roofs (Sinha et al. 1998; Carbotte et al. 2000; Singh et al. 2006) and the hundred-meters to kilometers-wide morphologic footprints of eruptive structures (e.g., Smith and Cann 1999; Smith et al. 1995). Smaller features, such as flat-topped volcanoes (e.g., 1-2 km across; Clague et al., 2000), can be reliable indicators for a heat source. However, current understanding of the coupled interaction between these features and ore-forming vent sites at MORs is not as developed as for large-scale geological systems. For example, the cycles of magmatic construction and tectonic destruction affecting neo-volcanic zones at MORs (Parson et al. 1993; Wilcock and Delaney 1996) induce temporal and spatial variations in the hydrothermal heat flux. These cycles could be further considered to evaluate permissive tracts.

2.3. Exploration risk

In mineral deposit targeting the chance of finding new discoveries is referred to as the probability of geologic success (P_g) (Otis and Schneidermann 1997). Geological processes that lead to the formation of mineral resources can be assigned a probability value relative to their absence or presence (from 0 to 1 respectively), given the heat source (P_1), fluid pathways (P_2), trap site (P_3) and reservoir unit (P_4). The product of the attributed probabilities gives P_g (Otis and Schneidermann 1997):

$$P_g = P_1 * P_2 * P_3 * P_4$$

The chance for ore generation can be low if some of the geological factors supporting mineralization processes are not completely identified in the available data. Because the observation of such factors depends on the available geoscience data and considering that the quantity and quality of such data may change from place to place, different levels of exploration risk must be specified within each permissive tract or within each of the identified prospects. The exploration risk is equal to one minus the probability of geological success ($1 - P_g$). Although its analysis incorporates geological aspects (Otis and Schneidermann 1997), economic risks (e.g., exploration and operation costs, or other financial and political aspects; e.g., Jones and Hillis 2003; Schiozer et al. 2004; Suslick et al. 2009) may additionally change the permissive tract evaluation, but those are not covered by this study. Spatially, a permissive tract can be subdivided into low-, moderate- and high-risk domains (see examples from Grant et al. 1996

for petroleum exploration) describing whether sections of the permissive tract may or may not contain the mineral resource of interest (P_g being high or low respectively), or whether uncertainty prevails (P_g close to 0.5). Areas of lower exploration risk can be identified where geological factors coincide spatially. However, this concept depends on the maximum risk acceptance decided by the investigator, i.e. if an exploration company has some history of drilling with a maximum risk of 0.30, then it may plan to continue exploration with an overall risk below that level. In addition, if a geological factor is absent within the region evaluated, P_g would be zero (high risk) because one geological factor will rank 0 in the analysis.

Evaluating the risk of exploring mineral deposits is a difficult exercise since it requires a certain expertise from the geoscientist(s) to evaluate the environments to be explored. The decision to pursue an exploration project is not only dependent on the calculation of P_g , but also on (1) the choice of the explorer to involve appropriate (and independent) geological factors in the overall evaluation and (2) how the probability of a mineral occurrence has been calculated (Milkov 2015). Because subjectivity is common in probability assessments (Baddeley et al. 2004), guidelines have been established for evaluating geological risk factors (e.g., Duff and Hall 1996; Otis and Schneidermann 1997; Rose, 2001). For example, Rose (2001) introduced a conceptual nomenclature to calibrate the probabilistic (and subjective) evaluation of geological factors. Critical processes may be evaluated to be either (i) present or more likely present (P_g between 0.6 and 1), (ii) significantly uncertain (0.4 to 0.6), (iii) less likely to be present (0.2 to 0.4), or (vi) nearly or completely absent (below 0.2). Because this classification does not take into account the various deposit types possibly described in a permissive tract (e.g., mafic-, ultramafic- and sediment-hosted deposits; Hannington et al. 2005), further conceptual thinking should integrate e.g., as formerly proposed by the U.S. Geological Survey (1991), (i) the likelihood of the presence of a resource given the environmental characteristics determined by e.g., geophysical and geological data, and (ii) a degree of confidence on the rating of resource potential, given the evidence or absence of e.g., specific rock units, structures and ore-forming processes. This division of subjective judgement, translated into probability values, helps to manage the problem of quantifying risk and uncertainty. However, it does not replace professional judgment but supplements it to improve the evaluation of exploration projects. Other forms of risk modeling, such as risk tables (e.g., Milkov 2015), can aggregate various information about the depositional environment of mineral resources. These tables compare the existence and reliability of data with pre-established geological models. Such models are well characterized in the oil

and gas industry (e.g., trap configurations, depositional settings and source rock types; [Allen and Allen 2013](#)), but remain to be defined for the exploration of seabed minerals.

2.4. Risks related to permissive tracts and prospects

The risk evaluation of mineral potential is made at the permissive tract and prospect levels depending on P_g . The risk defined for a particular prospect is multiplied with the risk calculated for its respective permissive tract as both target features are established with same geological circumstances. For example, if P_g corresponds to 0.8 and 0.7 at the permissive tract and prospect levels respectively, then the total P_g for the evaluated prospect is 0.56. Since the estimate of P_g depends on the availability and observation of data, multiple exploration scenarios can be examined:

- a. If the permissive tract is confirmed to have at least one mineral deposit, then the permissive tract in question (and related prospect) is proved to contain the required geological factors to promote mineralization; P_g is thus equal to 1 at the permissive tract (and prospect) level.
- b. If the permissive tract consists of prospects that are not confirmed or directly observed to contain mineral resources (unproven prospects), then P_g is estimated given the geological features analyzed at the permissive tract and prospect levels.
- c. If no prospects can be described within a permissive tract, then some aspects of mineralization patterns (e.g., the natural variability in the distribution of hydrothermal venting and related sulfide accumulation; [Fouquet et al. 2010](#); [Hannington et al. 2010](#)) can be considered for the permissive tract evaluation. Notably, hydrothermal vents are not always associated with polymetallic sulfides, and the recurrence of such accumulation, documented from the InterRidge database¹, gives insights on the likelihood of their occurrence. According to the database, about 239 hydrothermal systems (confirmed) occur along mid-ocean ridges and back-arc spreading centers, of which 73 are associated to polymetallic sulfide deposits. Thereby, the probability that one or more new discoveries in an unexplored permissive tract is associated with accumulations of sulfide minerals is 0.31. This probability can be combined with the number of undiscovered mineral deposits estimated for an unexplored permissive tract; such estimates can be established using the three-part

¹ A global database of active submarine hydrothermal vent fields (<https://vents-data.interridge.org/>).

form of mineral resource assessment from [Singer \(1993\)](#) and [Singer and Menzie \(2010\)](#) (see section 2.5.1). The end purpose of this is to determine the likelihood of finding unknown ore occurrences inside a permissive tract for which related prospects cannot be identified nor described. Therefore, P_g would correspond to a certain value for the permissive tract given the analysis of related geological features, and 0.31 for the undiscovered prospects inside the permissive tract in question.

2.5. Resource quantification

2.5.1. Considerations

Within a permissive tract, exploration or exploitation opportunities (camps and prospects) are ranked depending on the occurrence of geological phenomena (risk assessment) and the mineral potential of target zones. If the existence of prospects is not determined, the permissive tract evaluation can be made using a pre-established deposit model. The deposit model, as conceived by the three-part form of quantitative assessment provided by [Singer \(1993\)](#) and [Singer and Menzie \(2010\)](#), aggregates various information on e.g., the spatial distribution, grade and tonnage of well-explored analogue deposits, to indicate the undiscovered resource potential in an area considered geologically permissive for the occurrence of the mineral deposit type sought. Prior to this research, [Juliani and Ellefmo \(2018\)](#) have adapted a density model to the neo-volcanic zones of an ultra-slow spreading system, while grade and tonnage models of volcanogenic massive sulfides (VMS) deposits, which are analogue to current deep-sea hydrothermal ores ([Galley et al. 2007](#)), are provided from [Mosier et al. \(2009\)](#). These models will be applied to the permissive tract of this study, which is considered geologically similar to that of the axial volcanic ridges formerly established in the research of [Juliani and Ellefmo \(2018\)](#).

The potential mineralization extent in a prospect observed at the seafloor (e.g., from the analysis of high-resolution multi-beam data or magnetic anomalies; [Lipton 2012](#)) can be used to approximate an ore volume with the help of the ratio of tonnes of ore per m² of seafloor. Seafloor massive sulfides at the Solwara 1 project in the Bismarck Sea ([Lipton 2008, 2012](#)), for example, have been thoroughly explored by drilling (146 holes, maximum depth of 20 m), and their surficial dimension is approximated to be 90,000 m² for 2.5 Mt of ore. This area-tonnage relationship gives a ratio of 27.7 t/m² that can be used to construct first-order tonnage estimates for SMS, as formerly expressed by

[Hannington et al. \(2010\)](#). Applying this ratio to undrilled prospects would in normal case disregard the underlying physical dimensions of the associated potential orebody, but, given the lack of drilling data among known SMS deposits, it is a reasonable substitute to the tonnage distribution provided from a deposit model.

Geologic studies of the seafloor can be carried out locally using e.g., a remotely operated vehicle (ROV) ([Yeo and Searle, 2013](#); [Ludvigsen et al., 2016](#)) on the basis of available multi-beam data that have been previously acquired and processed. However, because the overall mapped seafloor cannot be always visited, some areas remain under-explored. Yet, the morpho-structural description of such areas through high-resolution multi-beam data can reveal structures related to unproven prospects, i.e. prospects that are not confirmed or directly observed to contain mineral resources. For example, mound-like or cone-shaped structures are often characteristic traits of accumulated ores (e.g., [Hannington et al. 1998](#); [Jamieson et al. 2014](#); [Webber et al. 2015](#)), and features with similar characteristics on a high-resolution bathymetry map may represent interesting targets. Similarly, a detailed magnetic survey over massive sulfide bodies can reveal strong magnetic lows due to the destruction of magnetic minerals in the associated hydrothermal alteration halo (e.g., [Tivey et al. 1993](#); [Tivey and Johnson 2002](#)). The extent of such detection may serve as a basis to make an anticipated estimate of ore volume given the above-mentioned tonnage-surface ratio (27.7 t/m²). However, because a high degree of analytical uncertainty exists in many aspects of seafloor investigations (e.g., artifacts in bathymetry and missing beam data; [de Moustier and Kleinrock, 1986](#)), a risk evaluation of the quality of the data collected needs to be considered.

To summarize, a permissive tract evaluation requires (i) statistical distributions of number of unknown ore occurrences, deposit size and ore grade, and (ii) a probability of geologic success of 0.31 if available data are not sufficient to identify prospects of ore; otherwise, Pg is evaluated among the identified prospects. The calculation of ore volume is made possible using a tonnage model (provided from [Mosier et al. \(2009\)](#)) if no in-situ prospects are identified. Otherwise, the mineral potential of prospects is indicated by combining their extent with a tonnage-surface ratio. Then, prospects are ranked given their estimated ore volumes and exploration risks (calculated using Pg). Because permissive tracts and camps are ranked given these estimates, some of them might be disregarded for further exploration (or exploitation) activities if the estimated resources are below the expectations of the investigator.

2.5.2. Calculation

Since SMS deposits are usually expected to contain various mixtures of precious and base metals (e.g., Cu, Zn, Au, and Ag; Hannington et al. 2010), separate resource evaluations will be achieved for each of these metals. After establishing a risk model, volumetric calculations can be carried out stochastically at the permissive tract, camp or prospect level using conventional Monte Carlo techniques where the number of deposits, tonnages, and grades are repeatedly sampled (e.g., 10,000 times in this study) and multiplied to obtain metal endowments. The evaluated risk associated to the permissive tract or prospects is thereafter multiplied with the metal endowment to obtain a probabilistic (log-normal) distribution of in-place metal resources. The distribution is generated in a cumulative form to present expected amounts of undiscovered metals at various confidence intervals, i.e., 10th, 50th and 90th percentiles; the latter is the value below which 90% of the observations may be found. The overall estimation process is treated through the stochastic calculator GeoX². The process can be summarized as follow: the various unproven prospects in a camp are given (1) a risk value, according to in-situ investigations of the geology, (2) an approximated tonnage using the previously-mentioned ratio (27.7 t/m²), and (3) an associated log-normally distributed grade model. The Monte Carlo simulation then combines these variables to report distributions of risked ore volumes for each prospect. Depending on the estimated volumes, several prospects and, or, the camp itself can be disregarded if the range of resultant outcomes are not of economic interest or too risky to be considered.

3. Case study

In this research, the above-described multi-scale evaluation method is applied to the Mohns Ridge, an ultra-slow spreading MOR (15 to 16 mm/yr; Mosar et al., 2002) situated within the Norwegian-Greenland Sea. The ridge consists of a deep rifted axial zone associated with significant isolated neo-volcanic zones recognizable from their hummocky-type terrain and associated volcanic edifices (e.g., flat-topped volcanoes, conic or dome structures and eruptive fissures; e.g., Yeo et al. 2012, 2013; Yeo and Searle 2013). These volcanic zones often appear in the form of topographic highs or axial volcanic ridges (AVRs) generally marked by characteristic morphologies (e.g., dome-shaped axial volcanic ridges, grabens, horsts and tilted blocks; Géli et al. 1994; Dauteuil and Brun 1996), which

² A decision support software for risk, resource and economic evaluation of exploration projects, licensed by Schlumberger Ltd. (<https://www.software.slb.com/products/geox>).

relate to the interplay between variations in magma supply and tectonism. The Mohns Ridge has well-developed tectonic features defined by numerous faults within the ridge valley trend (see details in [Juliani and Ellefmo 2018](#)). Past exploration activities describe several SMS occurrences along the ridge (Pedersen et al. 2010), among which the Loki's Castle vent field is situated inside the graben of the northernmost AVR currently ongoing tectonism. For the purpose of this research, this AVR is considered as a permissive tract into which the likelihood of undiscovered ore volumes will be estimated from identified prospects. The permissive tract analysis is processed using (1) low-resolution multibeam data, which have been acquired by the Norwegian Petroleum Directorate (NPD) in collaboration with the Geological Institute of the Russian Academy of Sciences (GIN RAS; Fig.2), and (2) high-resolution imagery of the Loki's Castle deposit and related environment to map the prospects and camps (Fig.3); these imagery data were acquired during the MarMine cruise by the Norwegian University of Science and Technology (NTNU) ([Ludvigsen et al. 2016](#)).

4. Results

4.1. Risk mapping

The preliminary assessment of where heat, pathway, trap and reservoir coincide (Table 2 and 3; Fig.4) is based on the consideration that (i) the release of heat is equally dispersed within the study area (Fig.3), (ii) permeability is relatively high near fractures; distance buffers are implemented to outline the uncertain propagation and continuum of fractures and cracks because sediments, often obscure their footprints, (iii) reservoirs are likely to be present in the form of mound-type structures or within sediment masses, and (iv) traps are associated with these mound-type features; in-situ structural conditions, such as silica-cemented materials, talus slope and local depressions, associated with neighboring evidence of mass wasting, are useful indicators. Large-scale features, such as AVRs and faults, provide sufficient and compelling evidence for the existence of heat and pathways (i.e., respective chance factor is 0.9). However, it is not clear whether these features drive hydrothermal processes as fault or fracture zones can be sealed ([Schroeder et al. 2002](#); [Gillis 2003](#)) and, or, the evolution of the underlying magma source (and associated heat release) is in a waning or waxing stage ([Parson et al. 1993](#); [Wilcock and Delaney 1996](#)). More local basement structures, i.e. reservoir and trap, are less likely to occur with high degree of certainty (evaluated to be 0.8). However, these can be mapped by mound-shaped structures on the seafloor (Fig.3) which can be assumed to represent hypothetical ore accumulations. The seafloor extent of these potential ore accumulations is usually of

thousands of m² in this study, which necessarily involves trapping and sealing mechanisms to promote ore accumulation and preservation.

4.2. Volumetric calculations

Probabilistic assessment of potential in-place resources within the two camps are shown on Fig.5 and 6, and the amount of ore and metal in each prospect is presented in Table 4. Assessed individually, prospects may or may not be of economic interest; e.g., the average amount of metals in the prospects 1, 4 and 10 (i.e., 13 to 22 kt of metals) can be eventually drilled or exploited, while others (e.g., prospects 2, 3, 5, 6, 8 and 9; Table 4), which have relatively lower resource volumes (<5 kt), could be excluded. Taken together, however, the prospects in the camp 2 increase the total resource potential (Fig.5) because they are proximal to each other; this may change the final exploration or mining development strategy. In contrast, the resource distribution for the camp 1 is rather uniform because most of the variation is captured by the Loki's Castle prospect. Within the study area, the probability of finding economically viable ore resources (Fig.6) depends on the combining of estimated ore volumes and related exploration risks.

5. Discussion

5.1. Mineral system

Estimating mineral resources requires diverse geoscience knowledge as summarized in the mineral system description for the project area (Table 1). However, because ore-forming processes are part of more extensive (ridge-scale) geological systems, other exploration criteria, in addition to heat source, pathway, trap and reservoir as presented in this study (Table 2), could be integrated; e.g., the geodynamic setting, including the spreading rate, sedimentary influences and the regional source of metals (host-rock type), all of which have potential impact on the deposit grade and tonnage (Hannington et al. 2005; 2011). Furthermore, the evaluation framework may also require an understanding of these criteria temporally, because hydrothermal-vent systems often tend to (i) have intermittent activity over long lifespan (Lalou et al. 1995; Cherkashov et al. 2016), (ii) undergo periodical activity and compositional changes due to nearby geological processes, such as eruptive events (Haymon et al. 1993; Butterfield et al. 1997; Von Damm et al. 1995, 1997) or earthquake swarms (Lilley et al. 2003; Seyfried et al. 2003), and (iii) occur within a specific window of seafloor construction between magmatic and tectonic spreading (Wilcock and Delaney 1996). The conditional rules applied to each exploration criteria (Table 2) demonstrate the limitation of the

multi-scale evaluation method presented in this study. However, these criteria can be described in geological, but also geophysical, hydrographic and, or, geochemical data, as shown in the mineral system (Table 1). For this reason, more conditional rules, such as those proposed in Table 2, can be applied to identify metallogenic regions given available data. To refine and update these rules, future investigators may get inspiration from both the type of information and organizing scheme employed in the petroleum system to define source-reservoir-trap configurations for oil and gas exploration (Allen and Allen 2013).

5.2. Permissive tract and risk mapping

The study area presented in this research (Fig.3), encompasses only one type locality in a tectonically active terrain (i.e., a portion of AVR undergoing sparse volcanic activity). However, neo-volcanic zones can form complex networks of volcanic structures (e.g., Yeo et al. 2013) that may require geophysical investigation, such as magnetic and electromagnetic surveys, to assist and optimize the permissive tract evaluation. The risk mapping of a complex permissive tract addresses complex structures in the crust, and the probability of finding a mineral deposit increases where structures are favorable for ore genesis. In the situation where a range of multiple prospects and camps are identified, however, the risk that mineralization events will occur in such features can be interdependent. This is because hydrothermal sites can extend over large areas (90,000 m²; Lipton 2008) and sulfide mounds can be clustered in different zones (e.g., the inactive Mir and Alvin zones situated 1.5 km east of the TAG sulfide mounds; Rona et al. 1993). The risk dependency of target features (prospects and camps) would increase (or decrease) the chance of finding new mineral occurrences when targets are considered together. If a camp (or a prospect) is successful or unsuccessful in terms of discovery, then the probability of making discoveries in other camps of the same permissive tract is assumed to change correspondingly; this conditional probability is described by Bayesian theorems as shown from the CCOP³ guidelines for risk assessment of petroleum target zones. In this context, estimated ore volumes that do not consider risk dependencies, such as those presented in Fig.5 and 6, may be biased.

5.3. Volumetric calculations

In the absence of drilling data, first-order determinations of resource potential, that are made on the basis of bathymetric structures (Fig.3), are informative, but also raise a whole set of new questions regarding the deposit

³ Document available online at http://www.ccop.or.th/assets/publication_digital/2912004_4_pdf.pdf.

thickness or the depth of ore mineralization below the seafloor. Such an approach may be adequate if the resolution of bathymetric data allows to distinguish small-scale (at the centimetric level) features of hydrothermal vent fields, such as pinnacle-shaped sulfide structures, fractures and local mass movements of ore and, or, sedimentary materials (e.g., [Webber et al. 2015](#)). Detailed bathymetry, assisted by the acquired acoustical properties of seafloor (e.g., backscatter and hyperspectral imaging data; [Ludvigsen et al. 2016](#)) and video profiling of deposit morphologies, is also valuable for planning offshore geophysical surveys and selecting locations for drilling, especially if the prospects have been identified in areas more prone to sedimentation, landslides and tectonism (e.g., [Cannat et al. 2013](#)). However, a high-resolution bathymetry model cannot confirm alone the existence of a sulfide body and, in this case, geophysical exploration techniques can be used to supplement the analysis.

6. Conclusion

The method for multi-scale quantitative risk analysis presented in this research can be used as an alternative framework for the investigation of seabed minerals. The framework leads to a work flow where the permissive tract, the camp and the prospect form a basis for identifying prospective areas early in the life of resource evaluation. When analyzing a permissive tract, the description of exposed geological factors (i.e., heat source, pathway, trap and reservoir) helps identifying the exploration risk of areas of interest while grade-tonnage-density models allow an estimation of preliminary resource estimates. However, a fundamental part of assessing mineral resources requires to take prior considerations regarding e.g., the type of deposit being studied (mafic-, ultramafic- or sediment-hosted deposits) and the related geological system (neo-volcanic zones, sedimented abyssal plains or tectonically active regions of MORs). For this reason, the mineral system described for the project area must be chosen carefully. In addition, this study evaluates exploration risk without drilling data. These data are necessary to develop grade-tonnage models suitable for evaluating current findings at MORs, and they can be used to update both the resource potential and exploration risks in camps and, or, prospects where drilling has been conducted. If future companies aim to adjust grade-tonnage models for in-house assessment procedures prior to establishing mining activities, increasing attention should be given to drilling campaigns and related costs.

References

Allen, P. A., & Allen, J. R. (2013). Basin Analysis: Principles and Application to Petroleum Play Assessment (3rd Edition), John Wiley & Sons, Somerset, NJ, USA, 632p.

Attanasi, E. D., & Freeman, P. A. (2009). Economics of undiscovered oil and gas in the North Slope of Alaska; Economic update and synthesis: U.S. Geological Survey Open-File Report 2009-1112. Available online at: <https://pubs.usgs.gov/of/2009/1112/pdf/ofr2009-1112.pdf>

Baddeley, M. C., Curtis, A., Wood, R. (2004). An introduction to prior information from probabilistic judgements: elicitation of knowledge, cognitive bias and herding. In: Curtis, A., Wood, R. (Eds.), Geological Prior Information: Informing Science and Engineering. Geological Society, 239, 15-27.

Baker, E. T., & German, C. R. (2004). On the global distribution of hydrothermal vent fields. In Mid-Ocean Ridges: Hydrothermal Interactions Between the Lithosphere and Oceans (C. R. German et al., eds.). AGU Geophysical Monograph Series, 148, Washington.

Baker, E. T., McDuff, R. E., & Massoth, G. J. (1990). Hydrothermal Venting from the Summit of a Ridge Axis Seamount: Axial Volcano, Juan de Fuca Ridge. Journal of Geophysical Research, 95, 12,843-12,854.

Bani-Hassan, N., Iyer, K., Rüpke, L. H., & Borgia, A. (2012). Controls of bathymetric relief on hydrothermal fluid flow at mid-ocean ridges. Geochem. Geophys. Geosyst., 13, 5, 1525-2027.

Beaulieu, S. E., Baker, E. T., German, C. R., Maffei, A. (2013). An authoritative global database for active submarine hydrothermal vent fields. Geochem. Geophys. Geosy., 14, 4892-4905.

Bruvoll, V., Breivik, A. J., Mjelde, R., Pedersen, R. B. (2009). Burial of the Mohn-Knipovich seafloor spreading ridge by the Bear Island Fan: Time constraints on tectonic evolution from seismic stratigraphy, Tectonic of the Mohn/Knipovich Bend. Tectonics, 28, TC4001.

Butterfield, D. A., Jonasson, I. R., Massoth, G. J., Feely, R. A., Roe, K. K., Embley, R. E., Holden, J. F., McDuff, R. E., Lilley, M. D., & Delaney, J. R. (1997). Seafloor eruptions and evolution of hydrothermal fluid chemistry. *Phil. Trans. Roy. Society of London, A*, 355, 369-386.

Canavan, F. (1973). Notes on the terms 'stratiform', 'stratabound' and 'stratigraphic control' as applied to mineral deposits. *Australian Journal of Earth Sciences*, 19 (4), 543-546.

Cannat, M., Mangeney, A., Ondréas, H., Fouquet, Y., & Normand, A. (2013). High-resolution bathymetry reveals contrasting landslide activity shaping the walls of the Mid-Atlantic Ridge axial valley. *Geoch., Geoph., Geosyst.*, 14, 4, 996-1011, <http://dx.doi.org/10.1002/ggge.20056>.

Carbotte, S. M., Solomon, A., & Ponce-Correa, G. (2000). Evaluation of morphological indicators of magma supply and segmentation from a seismic reflection study of the East Pacific Rise 15°30'-17°N. *Journal of Geophysical Research*, 105 (B2), 2737-2759.

Caress, D. W., Thomas, H., Kirkwood, W. J., McEwen, R., Henthorn, R., Clague, D. A., Paull, C. K., Paduan, J., Maier, K. (2008). High-resolution multibeam, sidescan and subbottom surveys using the MBARI AUV D. Allan B. In: Reynolds JR, Greene HG (eds) *Marine habitat mapping technology for Alaska*. Alaska Sea Grant College Program, Fairbanks, 47-69.

Cherkashov, G., Kuznetsov, V., Kuksa, K., Tabuns, E., Maksimov, F., Bel'tenev, V. (2016). Sulfide geochronology along the Northern Equatorial Mid-Atlantic Ridge. *Ore Geology Review*, 87, 147-154.

Cherkashov, G., Bel'tenev, V., Ivanov, V., Lazareva, L., Samovarov, M., Shilov, V., Stepanova, T., Glasby, G. P., Kuznetsov, V. (2008). Two New Hydrothermal Fields at the Mid-Atlantic Ridge. *Mar. Georesources Geotechnol.*, 26, 308-316, <https://doi:10.1080/10641190802400708>.

Clague, J. J., & Stead, D. (2012). *Landslides: types, mechanism and modeling*. Cambridge University Press, 345-358.

Clague, D. A., Moore, J. G. and Reynolds, J. R., 2000. Formation of submarine flat-topped volcanic cones in Hawai'i. *Bulletin of Volcanology*, 62 (3), 214-233.

Cox, D. P., & Singer, D. A. (1986). *Mineral deposit models*: U.S. Geological Survey Bulletin 1693, 318-348.

Curewitz, D., & Karson, J. A. (1997). Structural settings of hydrothermal outflow: Fracture permeability maintained by fault propagation and interaction. *J. Volcanol. Geotherm. Res.*, 79(3-4), 149-168.

Dauteuil, O., & Brun, J. P. (1996). Deformation partitioning in a slow spreading ridge undergoing oblique extension: Mohns Ridge, Norwegian Sea. *Tectonics*, 15, 870-884.

Davis, E. E., Mottl, M. J., Fisher, A. T., et al. (1992). *Proceedings of the Ocean Drilling Program, Initial Reports*, 139, 1026 pp., Ocean Drill. Program, College Station, Tex.

Delaney, J. R., Robigou, V., McDuff, R. E., & Tivey, M. K. (1992). Geology of a vigorous hydrothermal system on the Endeavour segment, Juan de Fuca Ridge. *Journal of Geophysical Research*, 97, 19,663-19,682.

deMartin, B. J., Sohn, R. A., Canales, J. P., & Humphris, S. E. (2007). Kinematics and geometry of active detachment faulting beneath the Trans-Atlantic Geotraverse (TAG) hydrothermal field on the Mid-Atlantic Ridge, *Geology*, 35, 711-714.

de Moustier, C. & Kleinrock, M. C. (1986). Bathymetric artifacts in Sea Beam data: how to recognize them and what causes them. *J. Geophys. Res.*, 91, 3407-3424.

Dick, H. J. B., Natland, J. H., Alt, J. C., Bach, W., Bideau, D., Gee, J. S., Haggis, S., Hertogen, J., Hirth, G., Holm, P. M., Ildfonse, B., Iturrino, G. J., John, B. E., Kelley, D. S., Kikawa, E., Kingdon, A., Le Roux, P. J., Maeda, J., Meyer, P. S., Miller, D. J., Naslund, H. R., Niu, Y.-L., Robinson, P. T., Snow, J., Stephen, R. A., Trimby, P. W., Worm, H.-U., & Yoshinobu, A. (2000). A long in-situ section of the lower ocean crust: Results of ODP Leg 176 drilling at the Southwest Indian Ridge. *Earth Planet. Sci. Lett.*, 179, 31-51.

Duff, B. A. & Hall, D. (1996). A model-based approach to evaluation of exploration opportunities. In: *Quantification and Prediction of Petroleum Resources* edited by A.G. Doré and R. Sinding-Larsen. NPF Special Publication 6, 183-198, Elsevier, Amsterdam.

Dutton, S. P., Kim, E. M., Broadhead, R. F., Raatz, W., Breton, C., Ruppel, S. C., Kerans, C., & Holtz, M. H. (2003). *Play analysis and digital portfolio of major oil reservoirs in the Permian Basin: Application and transfer of advanced geological and engineering technologies for incremental production opportunities*. The University of Texas at Austin, Bureau of Economic Geology, and New Mexico Bureau of Geology and Mineral Resources, New Mexico Institute of Mining and Technology, annual report prepared for U.S. Department of Energy. Available online at: <https://www.osti.gov/servlets/purl/825581>

Dvorak, D. H., Hedin, R. S., Edenborn, H. M., & McIntire, P. E. (1992). Treatment of metal-contaminated water using bacterial sulfate reduction: results from pilot-scale reactors. *Biotechnol. Bioeng.*, 40, 609-616.

Ehrlich, H. L. (1999). Microbes as geologic agents: Their role in mineral formation. *Geomicrobiol J.*, 16, 135-153.

Escartin, J., Smith, D. K., Cann, J., Shouten, H., Langmuir, C. L., & Escrig, S. (2008). Central role of detachment faults in accretion of slow spreading oceanic lithosphere. *Nature*, 455, 790-794.

Ferrario, A., & Garuti, G. (1980). Copper deposits in the basal breccias and volcano-sedimentary sequences of the eastern Ligurian ophiolites (Italy). *Min. Deposits*, 15, 291-303.

Firstova, A., Stepanova, T., Cherkashov, G., Goncharov, A., & Babaeva, S. (2016). Composition and formation of gabbro-peridotite hosted seafloor massive sulfide deposits from the Ashadze-1 hydrothermal field, Mid-Atlantic Ridge. *Minerals* 2016, 6 (19).

Fisher, A. T., Becker, K., & Narasimhan, T. N. (1994). Off-axis hydrothermal circulation: parametric tests of a refined model of processes at Deep Sea Drilling Project/Ocean Drilling Program site 504. *J. Geophys. Res.*, 99, 3097-3121.

Fouquet, Y., Cambon, P., Etoubleau, J., Charlou, J. L., Ondreas, H., Barriga, F. J. A. S., Cherkashov, G., Semkova, T., Poroshina, I., Bohn, M., Donval, J. P., Henry, K., Murphy, P., Rouxel, O. (2010). Geodiversity of hydrothermal processes along the Mid-Atlantic Ridge and ultramafic-hosted mineralization: A new type of oceanic Cu-Zn-Co-Au volcanogenic massive sulfide deposit. Article in *Geophysical Monograph Series*, 188, 321-367.

Fouquet, Y., Zierenberg, R. A., Miller, D. J., Bahr, J. M., Baker, P. A., Bjerkgård, T., Brunner, C. A., Duckworth, R. C., Gable, R., Gieskes, J., Goodfellow, W. D., Gröschel-Becker, H. M., Guèrin, G., Ishibashi, J., Iturrino, G., James, R. H., Lackschewitz, K. S., Marquez, L. L., Nehlig, P., Peter, J. M., Rigsby, C. A., Schultheiss, P., Shanks, W. C., III, Simoneit, B. R. T., Summit, M., Teagle, D. A. H., Urbat, M., Zuffa, G. G. (1998). Investigation of hydrothermal circulation and genesis of massive sulfide deposits at sediment-covered spreading centers at Middle Valley and Escanaba trough: Proceedings of the Ocean Drilling Program, Initial Reports, 169, 7-16.

Fouquet, Y., Wafik, A., Cambon, P., Mevel, C., Meyer, G., & Gente, P. (1993). Tectonic setting and mineralogical and geochemical zonation in the Snakepit sulphide deposit (Mid-Atlantic Ridge at 23°N). *Econ. Geol.*, 88, 2018-2036.

Fouquet, Y., Auclair, G., Cambon, P., & Etoubleau, J. (1988). Geological setting and mineralogical and geochemical investigations on sulfide deposits near 13°N on the East Pacific Rise. *Mar. Geol.*, 84, 143-178.

Galley, A. G., Hannington, M., Jonasson, I. (2007). Volcanogenic massive sulphide deposits. In: Goodfellow WD, ed., Mineral deposits of Canada - A synthesis of major deposit-types, district metallogeny, the evolution of geological provinces, and exploration methods. Geological Association of Canada, Mineral Deposits Division, Special Publication, 5, 141-161.

Garuti, G., Alfonso, P., Zaccarini, F., & Proenza, J. A. (2009). Sulfur-isotope variations in sulfide minerals from massive sulfide deposits of the northern Apennine ophiolites: inorganic and biogenic constraints. *Ofioliti*, 34, 43-62.

Garuti, G., Bartoli, O., Scacchetti, M., Zaccarini, F. (2008). Geological setting and structural styles of Volcanic Massive Sulfide deposits in the northern Apennines (Italy): evidence for seafloor and subseafloor hydrothermal activity in unconventional ophiolites of the Mesozoic Tethys. *Bol. Soc. Geol. Mexicana*, 60, 121-145.

Garuti, G., & Zaccarini, F. (2005). Minerals of Au, Ag And U in volcanic-rock-associated massive sulfide deposits of the Northern Apennine Ophiolite (Italy). *Canadian mineralogist*, 43, 935-950.

Gautier, D. L., Dolton, G. L., Takahashi, K. I., & Varnes, K. L. (1995). National assessment of US oil and gas resources. Overview of the 1995 national assessment. Results, methodology, and supporting data: US Geological Survey Digital Data Series 30 (available online).

Géli, L., Renard, V., Rommevaux, C. (1994). Ocean crust formation processes at very slow spreading centers: A model for the Mohns Ridge, near 72°N, based on magnetic, gravity, and seismic data. *Journal of Geoph. Res.*, 99, 2995-3013.

German, C. R., & Von Damm, K. L. (2004). Hydrothermal processes. In: Holland, H.D., Turekian, K.K. & Elderfield, H. (eds.) *Treatise on geochemistry*, Vol. 6. The oceans and marine geochemistry. Oxford, UK, Elsevier-Pergamon, 181-222.

Gillis, K. M. (2003). Subseafloor geology of hydrothermal root-zones at oceanic spreading centers, in *Energy and Mass Transfer in Marine Hydrothermal Systems*, edited by Halbach, P. E., Tunncliffe, V., & Hein, J. R., 53-70, Dahlem. Univ. Press, Berlin.

Gràcia, E., Bideau, D., Hekinian, R., Lagabfielle, Y., & Parson, L. M. (1997). Along-axis magmatic oscillations and exposure of ultramafic rocks in a second-order segment of the Mid-Atlantic Ridge (33 °43'N to 34 °07'N). *Geology*, 25, 1059-1062.

Grant, S., Milton, N., & Thompson, M. (1996). Play fairway analysis and risk mapping: an example using the Middle Jurassic Brent Group in the northern North Sea. In: *Quantification and Prediction of Petroleum Resources*, Doré, A. G. and Sinding-Larsen, R. eds., NPF Special Publication, 6, 167-181, Elsevier.

Hall, J. M., & Yang, J. S. (1994). A preferred environment of preservation for volcanic massive sulfide deposits in Troodos Ophiolite (Cyprus). *Economic Geology*, 89, 851-857.

Hagemann, S. G., Lisitsin, V. A., & Huston, D. L. (2016). Mineral System. Analysis: Quo Vadis. *Ore geology Reviews*, 76, 504-22.

Hannington, M. D., Jamieson, J., Monecke, T., Petersen, S., & Beaulieu, S. (2011). The abundance of seafloor massive sulfide deposits. *Geology*, 39(12), 1155-1158.

Hannington, M. D., Jamieson, J., Monecke, T., Petersen, S. (2010). Modern sea-floor massive sulfides and base metal resources: toward an estimate of global sea-floor massive sulfide potential. *Spec. Publ. Soc. Econ. Geol.*, 15, 317-338.

Hannington, M. D., de Ronde, C. E. J., & Petersen, S. (2005). Sea-floor tectonics and submarine hydrothermal systems. In: Hedenquist, J. W., Thompson, J. F. H., Goldfarb, R. J., and Richards, J. P., eds, *Economic Geology One Hundredth Anniversary Volume: Society of Economic Geologists*, 111-141.

Hannington, M. D., Galley, A. G., Herzig, P. M., & Petersen, S. (1998). Comparison of the TAG mound and stockwork complex with Cyprus-type massive sulphide deposits, in *Proceedings of the Ocean Drilling Program, Scientific Results*, 158, 389-415.

Haymon, R., Fornari, D., Von Damm, K., Lilley, M. D., Perfit, M. R., Edmond, J. M., Shaks, W. C., Lutz, R. A., Grebmeier, J. M., Carbotte, S., Wright, D., McLaughlin, E., Smith, M., Beedle, N., & Olson, E. (1993). Volcanic eruption of the mid-ocean ridge along the East Pacific Rise at 9°45-52'N: Direct submersible observation of seafloor phenomena associated with an eruption event in April 1991. *Earth Planet. Sci. Lett.*, 119, 85-101.

Honsho, C., Ura, T., Asada, A., Kim, K., & Nagahashi, K. (2015). High-resolution acoustic mapping to understand the ore deposit in the Bayonnaise knoll caldera, Izu-Ogasawara arc. *Journal of Geophysical Research, Solid Earth*, 120, 2070-2092.

Hronsky, J. M. A., & Groves, D. (2008). Science of targeting: definition, strategies, targeting and performance measurement. *Australian Journal of Earth Sciences*, 55, 3-12.

Humphris, S. E., Fornari, D., Scheirer, D., German, C. R., & Parson, L. M. (2002). Geotectonic setting of hydrothermal activity on the summit of Lucky Strike Seamount (37°17'N) (Mid-Atlantic Ridge). *Geochem. Geophys. Geosyst.*, 3(8).

Jamieson, J. W., Clague, D. A. & Hannington, M. D. (2014). Hydrothermal sulfide accumulation along the Endeavour Segment, Juan de Fuca Ridge. *Earth and Planetary Science Letters*, 395, 136-148.

Johnson, H. P., Karsten, J. L., Vine, F. J., Smith, G. C., & Schonharting, G. (1982). A low-level magnetic survey over a massive sulfide ore body in the Troodos ophiolite complex, Cyprus. *Marine Technology Society Journal*, 16.

Jones, R. M., Hillis, R. R. (2003). An integrated, quantitative approach to assessing fault-seal risk. *AAPG Bulletin*, 87, 507-24. *Earth-Science Reviews*, 150, 453-476.

Juliani, C., Ellefmo, S. L. (2018). Probabilistic estimates of permissive areas for undiscovered seafloor massive sulfide deposits on an Arctic Mid-Ocean Ridge. *Ore Geology Reviews*, 95, 917-930.

Kawada, Y., & Kasaya, T. (2017). Marine self-potential survey for exploring seafloor hydrothermal ore deposits. *Scientific Reports*, 7.

Karson, J. A., & Rona, P. A. (1990). Block-tilting, transfer faults and structural control of magmatic and hydrothermal processes in the TAG area, Mid-Atlantic Ridge 26°N. *Geological Society of America Bulletin*, 102, 1635-1645.

Kent, G. M., Singh, S. C., Harding, A. J., Sihna, M. C., Orcutt, J. A., Barton, P. J., White, R. S., Bazin, S., Hobbs, R. W., Tong, C. H., & Pye, J. W. (2000). Evidence from three-dimensional seismic reflectivity images for enhanced melt supply beneath mid-ocean ridge discontinuities. *Nature*, 406, 614-618.

Knox-Robinson, C., & Wyborn, L. A. I. (1997). Towards a holistic exploration strategy: using geographic information systems as a tool to enhance exploration. *Australian Journal of Earth Sciences*, 44, 453-463.

Koski, R. A., Benninger, L. M., Zierenberg, R. A., Jonasson, I. R. (1994). Composition and growth history of hydrothermal deposits in Escanaba Trough, southern Gorda Ridge. In: Morton, J.L., Zierenberg, R.A., Riess, C.A. (Eds.), *Geologic, Hydrothermal, and Biologic Studies at Escanaba Trough, Gorda Ridge, Offshore Northern California*. U.S. Geol. Surv. Bull., 2022, 293-324.

Koski, R. A., Shanks, W. C., III, Bohrson, W. A., & Oscarson, R. L. (1988). The composition of massive sulfide deposits from the sediment-covered floor of Escanaba Trough, Gorda Ridge: implications for depositional processes. *Can. Mineral*, 26, 655-673.

Koski, R. A., Lonsdale, P. F., Shanks, W. C., Berndt, M. E., & Howe, S. S. (1985). Mineralogy and geochemistry of a sediment hosted hydrothermal sulfide deposit from the southern trough of Guaymas basin, Gulf of California. *J. Geophys. Res.*, 90, 6695-6707.

Labrenz, M., Druschel, G. K., Thomsen-ebert, T. et al. (2000). Formation of sphalerite (ZnS) deposits in natural biofilms of sulfate-reducing bacteria. *Science*, 290, 1744–1747.

Lalou, C., Reyss, J. L., Brichet, E., Rona, P. A., & Thompson, G. (1995). Hydrothermal activity on a 10⁵-year scale at a slow-spreading ridge. TAG hydrothermal field, Mid-Atlantic Ridge 26°N. *Journal of Geophysical Research*, 100, 17,855-17,862.

Langmuir, C. H., Humphris, S., Fornari, D., Van Dover, C., Von Damm, K., Tivey, M. K., Colodner, D., Charlou, J.-L., Desonie, D., Wilson, C., Fouquet, Y., Klinkhammer, G., & Bougault, H. (1997). Hydrothermal vents near a mantle hot-spot: the Lucky Strike vent field at 37°N on the Mid-Atlantic Ridge. *Earth Planet. Sci. Lett.*, 148, 69-91.

Lavier, L., Buck, W. R., & Poliakov, A. (1999). Self-consistent rolling-hinge model for the evolution of large-onset low-angle normal faults. *Geology*, 27, 1127-1130.

Lawson, K., Searle, R. C., Pearce, J. A., Browning, P., & Kempton, P. (1996). Detailed volcanic geology of the MARNOK area, Mid-Atlantic Ridge north of Kane transform. In: *Tectonic, Magmatic, Hydrothermal and Biological Segmentation of Mid-Ocean Ridges*, 118, edited by C. J. MacLeod, P. A. Tyler, & C. L. Walker, 61-102, Geol. Soc., London, U.K.

Lilley, M. D., Butterfield, D. A., Lupton, J. E., & Olson, E. J. (2003). Magmatic events can produce rapid changes in hydrothermal vent chemistry. *Nature*, 422, 878-881.

Lipton, I. L. (2012). Mineral Resource Estimate, Solwara 1 Project, Bismark Sea, Papua New Guinea. Technical Report compiled under NI140-101, 1-240.

Lipton, I. (2008). Mineral resource estimate, Solwara 1 project, Bismarck Sea, Papua New Guinea: Canadian NI 43-101 Technical Report for Nautilus Minerals Inc., 277p.

Lisitsyn, A. P., Bogdanov, Y. A., Zonenshayn, L. P., Kuz'min, M. I., & Sagalevich, A. M. (1989). Hydrothermal phenomena in the Mid-Atlantic Ridge at Lat. 26°N (TAG hydrothermal field). *Int. Geol. Rev.*, 31, 1183-1198.

Ludvigsen, M., Aasly, K., Ellefmo, S. L., Hilário, A., Ramirez-Llodra, E., Søreide, F. X., Falcon-Suarez, I., Juliani, C. J., Kieswetter, A., Lim, A., Christian, M., Nornes, S. M., Reimers, H., Paulsen, E., Sture, Ø. (2016). MarMine cruise report: Arctic Mid-Ocean Ridge 15.08.2016 - 05.09.2016. Available online: <https://brage.bibsys.no/xmlui/handle/11250/2427715>.

McAllister, E., & Cann, J. (1996). Initiation and evolution of boundary wall faults along the Mid-Atlantic Ridge, 25-29°N. In: MacLeod, C. J., Tyler, P. A. & Walker, C. L. (eds) 1996, *Tectonic, Magmatic, Hydrothermal and Biological Segmentation of Mid-Ocean Ridges*. Geological Society Special Publication, 118, 29-48.

McCaig, A. M., Cliff, R. A., Escartin, J., Fallick, A. E. & MacLeod, C. J. (2007). Oceanic detachment faults focus very large volumes of black smoker fluid. *Geology*, 35, 935-938.

McCuaig, T. C., Hronsky, J. M. A. (2014). The mineral system concept: the key to exploration targeting. *Society of Economic Geologists Special Publication*, 18, 153-175.

Melchert, B, Devey C. W., German, C. R., Lackschewitz, K. S., Seifert, R., Walter, M., Mertens, C., Yoerger, D. R., Baker, E. T., Paulick, H., Nakamura, K. (2008). First evidence for high-temperature off-axis venting of deep crustal/mantle heat: The Nibelungen hydrothermal field, southern Mid-Atlantic Ridge. *Earth Planet. Sci. Lett.*, 275(1-2), 61-69.

Milkov, A. V. (2015). Risk tables for less biased and more consistent estimation of probability of geological success (pos) for segments with conventional oil and gas prospective resources. *Earth-Science Reviews*, 150, 453-476.

Miller, K. A., Thompson, K. F., Johnston, P., & Santillo, D. (2018). An overview of seabed mining including the current state of development, environmental impacts and knowledge gaps. *Front. Mar. Sci.*, 4, 418.

Mills, R. A., Tivey, M. K. (1999). Sea water entrainment and fluid evolution within the TAG hydrothermal mound: evidence from analyses of anhydrite. In: Cann, J. R., Elderfield, H., Laughton A. (Eds.), *Mid-Ocean Ridges*. The Royal Society, Cambridge, 225-263.

Mills, R. A., Teagle, D. A. H., & Tivey, M. K. (1998). Fluid mixing and anhydrite precipitation within the TAG mound. In *Proceedings from the Oceanic Drilling Program Scientific Results*, ed. P. M. Herzig, S. E. Humphris, D. J. Miller, & R. A. Zierenberg. College Station, Texas, 158, 119-27.

Mosar, J., Lewis, G. & Torsvik, T. H. (2002). North Atlantic sea-floor spreading rates: implications for the Tertiary development of inversion structures of the Norwegian–Greenland Sea. *J. of the Geol. Soc., London*, 159, 503-515.

Mosier, D. L., Berger, V. I., & Singer, D. A. (2009). *Volcanogenic Massive Sulfide Deposits of the World: Database and Grade and Tonnage Models*. Open-File Report 2009-1034, U.S. Department of the Interior/U.S. Geological Survey, 50p.

Murton, B. J., & Rona, P. A. (2015). Carlsberg Ridge and Mid-Atlantic Ridge: comparison of slow-spreading centre analogues. *Deep Sea Research II, Topical studies in Oceanography*, 32, 71-84.

Mutton B. J., Klinkhammer, G., Becker, K., Briais, A., Edge, D., Hayward, N., Millard, N., Mitchell, I., Rouse I., Rudnicki, M., Sayanagi, K., Sloan, H., & Parson, L. (1994). Direct measurements of the Distribution and Occurrence

of Hydrothermal Activity Between 27 and 30 degrees north on the Mid-Atlantic Ridge. *Earth Planer. Sci. Lett.* 125, 119-128.

Norwegian Petroleum Directorate (NPD) 2017. The Shelf in 2017. Available online at:

<http://www.npd.no/Global/Engelsk/1-Whats-new/News/The-Shelf-2017/Sokkelaret2017-samlet-E.pdf>

Ondréas, H., Cannat, M., Fouquet, Y., Normand, A., Sarradin, P. M., & Sarrazin, J. (2009). Recent volcanic events and the distribution of hydrothermal venting at the Lucky Strike hydrothermal field, Mid-Atlantic Ridge, *Geochem. Geophys. Geosyst.*, 10, Q02006. doi:10.1029/20086C002171

Otis, R. M., Schneidermann, N. (1997). A process for evaluating exploration prospects. *AAPG Bull.* 81, 1087-1109.

Parsons, T., & Thompson, G. A. (1993). Does magmatism influence low-angle normal faulting? *Geology*, 21, 247-250.

Pedersen, R. B., Thorseth, I. H., Nygård, T. E., Lilley, M. D., Kelley, D. S. (2010). Hydrothermal activity at the Arctic Mid-Ocean Ridges, in: Rona, P. A., Devey, C. W., Dymont, J., Murton, B. J. (Eds.), *Geophysical Monograph Series*. American Geophysical Union, Washington, D.C., 67-89.

Petersen, S., Kuhn, L., Kuhn, T., Augusting, N., Hekinian, R., Franz, L., & Borowski, C. (2009). The geological setting of the ultramafic-hosted Logatchev hydrothermal field (14°45'N, Mid-Atlantic Ridge) and its influence on massive sulfide formation. *Lithos*, 112, 40-56.

Reed, M. H., & Palandri, J. (2006). Sulfide Mineral Precipitation from Hydrothermal Fluids. *Reviews in Mineralogy and Geochemistry*, 61, 609-631.

Reston, T. J., & Ranero, C. R. (2011). The 3-D geometry of detachment faulting at mid-ocean ridges. *Geochemistry, Geophysics, Geosystems*, 12 (7), Q0AG05.

Rona, P. A., Hannington, M. D., Raman, C. V., Thompson, G., Tivey, M. K., Humphris, S. E., Lalou, C., & Petersen, S. (1993). Active and relict seafloor hydrothermal mineralization at the TAG hydrothermal field, Mid-Atlantic Ridge. *Econ. Geol.*, 88, 1987-2013.

Rose, P. R. (2001). Risk analysis and management of petroleum exploration ventures. *AAPG Methods in Exploration Series*, 12, 164 p.

Rubin, K. H., Soule, S. A., Chadwick, W. W., Fornari, D. J., Clague, D. A., Embley, R. W., Baker, E. T., Perfit, M. R., Caress, D. W., & Dziak, R. P. (2012). Volcanic eruptions in the deep sea. *Oceanography* 25, 142-157.
doi:10.5670/oceanog.2012.12

Rubin, A. M. (1992). Dike-induced faulting and graben subsidence in volcanic rift zones. *J. Geophys. Res.*, 97, 1839-1858.

Rubin, A. M., & Pollard, D. D. (1988). Dike-induced faulting in rift zones of Iceland and Afar. *Geology*, 16, 413-417.

Scheirer, D. S., Macdonald, K. C. (1993). Variation in cross-sectional area of the axial ridge along the East Pacific Rise: Evidence for the magmatic budget of a fast spreading center. *J. Geophys. Res.*, 98, 7871-7885.

Schiozer, D. J., Ligerio, E. L., & Santos, J. A. M. (2004). Risk assessment for reservoir development under uncertainty. *Journal of the Brazilian Society of Mechanical Sciences and Engineering*, 26 (2), 213-217.

Schindwein, V., Demuth, A., Korger, E., Läderach, C., & Schmid, F. (2015). Seismicity of the Arctic mid-ocean ridge system. *Polar Science*, 9 (1), 146-157.

Schroeder, T., John, B. E., & Frost, B. R. (2002). Geologic implications of seawater circulation through peridotite exposed at slow spreading mid-ocean ridges. *Geology*, 30, 367-370.

Seyfried, W. E., Seewald, J. S., Berndt, M. E., Ding, K., & Foustoukos, D. I. (2003). Chemistry of hydrothermal vent fluids from the Main Endeavour Field, northern Juan de Fuca Ridge: Geochemical controls in the aftermath of June 1999 seismic events. *Journal of Geophysical Research*, 108, B9 2429. doi: 10.1029/2002JB001957

Singer, D. A., Menzie, W. D. (2010). *Quantitative Mineral Resource Assessments, an Integrated Approach*. Oxford University Press.

Singer, D. A. (2008). Mineral deposit densities for estimating mineral resources. *Math. Geosci.*, 40, 33-46.

Singer, D. A. (1993). Basic concepts in three-part quantitative assessments of undiscovered mineral resources. *Non-Renewable Resources*, 2 (2), 69-81.

Singh, S. C., Crawford, W. C., Carton, H., Seher, T., Combier, V., Cannat, M., Canales, J. P., Dusunur, D., Escartin, J., Miranda, J. W. (2006). Discovery of a magma chamber and faults beneath Mid-Atlantic Ridge hydrothermal field. *Nature*, 442, 1029-1032.

Sinha, M., Constable, S., Peirce, C., White, A., Heinson, G., MacGregor, L., Navin, D. (1998). Magmatic processes at slow spreading ridges: implications of the RAMESSES experiment at 57°45'N on the Mid-Atlantic Ridge. *Geophys. J. Int.*, 135(3), 731-745.

Smith, D. K., Escartin, J., Schouten, H., & Cann, J. R. (2008). Fault rotation and core complex formation: Significant processes in seafloor formation at slow-spreading mid-ocean ridges (Mid-Atlantic Ridge, 13°-15°N). *Geochemistry Geophysics Geosystems*, 9, Q03003. doi: 10.1029 /2007GC001699

Smith, D. K., & Cann, J. R. (1999). Constructing the upper crust of the Mid-Atlantic Ridge: a reinterpretation based on Puna Ridge, Kilauea Volcano. *Journal of Geophysical Research*, 104, 25,379-25,399.

Smith, D. K., Humphris, S. E., & Bryan, W. B. (1995). A comparison of volcanic edifices at the Reykjanes Ridge and the Mid-Atlantic Ridge at 24°-30°N. *Journal of Geophysical Research*, 100 (B11), 22,485-22,498.

Smith, D. K., & Cann, J. R. (1990). Hundreds of small volcanoes on the median valley floor of the Mid-Atlantic Ridge at 24°30'N. *Nature*, 348, 152-155.

Sørensen, M. B., Ottemoller, L., Havskov, J., Atakan, K., Hellevang, B. & Pedersen, R. B. (2007). Tectonic processes in the Jan Mayen fracture zone based on earthquake occurrence and bathymetry. *Bulletin of the Seismological Society of America*, 97, 772-779.

Suslick, S. B., Shiozer, D., Rodrigues, M. R. (2009). Uncertainty and risk analysis in petroleum exploration and production. *TERRÆ*, 3(2), 36-47.

Tivey, M. A., & Johnson, H. P. (2002). Crustal magnetization reveals subsurface structure of Juan de Fuca Ridge hydrothermal vent fields. *Geology*, 30, 979-982.

Tivey, M. K., Mills, R. A., Teagle, D. A. H. (1998). Temperature and salinity of fluid inclusions in anhydrite as indicators of seawater entrainment and heating in the TAG active mound, in Herzig, P. M., Humphris, S. E., et al., eds., *Proceedings of the Ocean Drilling Program. Scientific Results*, 158: College Station, Texas. Ocean Drilling Program, 179-190.

Tivey, M. K., Humphris, S. E., Thompson, G., Hannington, M. D., Rona, P. A. (1995). Deducing patterns of fluid flow and mixing within the active TAG mound using mineralogical and geochemical data. *J. Geophys. Res.* 100, 12,527-12,555. doi:10.1029/95JB00610

Tivey, M. A., Rona, P. A., & Schouten, H. (1993). Reduced crustal magnetization beneath the active sulfide mound, TAG hydrothermal field, Mid-Atlantic Ridge 26°N. *Earth Planet. Sci. Lett.*, 115, 101-115.

Tolstoy, M., Waldhauser, F., Bohnenstiehl, D. R., Weekly, R. T., Kim, W. Y. (2008). Seismic identification of along-axis hydrothermal flow on the East Pacific Rise. *Nature*, 451, 181-184.

Tucholke, B. E., Behn, M. D., Buck, W. R., & Lin, J. (2008). Role of melt supply in oceanic detachment faulting and formation of megamullions. *Geology*, 36, 455-458.

U.S. Department of the Interior and U.S. Geological Survey 1991. Mineral Reserves, Resources, Resource Potential, and Certainty, 95-97. In: *Suggestions to Authors of the Reports of the United States Geological Survey*, 7th edition, Washington, US Government Printing Office. Available online at: <http://www.nwrc.usgs.gov/techrpt/sta13.pdf>

Von Damm, K. L., Buttermore, L. G., Oosting, S. E., Bray, A. M., Fornari, D. J., Lilley, M. D., Shanks, III, W. C. (1997). Direct observation of the evolution of a seafloor “black smoker” from vapor to brine. *Earth and Planet Sci. Lett.*, 149, 101-111.

Von Damm, K. L. (1995). Controls on the chemistry and temporal variability of seafloor hydrothermal fluids. *Geophys. Monogr. (AGU)* 91, 222-247.

Walker, S. L., Baker, E. T., Massoth, G. J., & Hey, R. N. (2004). Short-term variations in the distribution of hydrothermal plumes along a superfast spreading center, East Pacific Rise, 27°30′-32°20′S, *Geochem. Geophys. Geosyst.*, 5, Q12005. doi:10.1029/2004GC000789

Webber, A. P., Roberts, S., Murton, B. J., Hodgkinson, M. R.S. (2015). Geology, sulfide geochemistry and supercritical venting at the Beebe Hydrothermal Vent Field, Cayman Trough. *Geochem. Geophys. Geosyst.*, 16, 2661-2678.

Wheeler, A. J., Murton, B., Copley, J., Lim, A., Carlsson, J., Collins, P., Dorschel, B., Green, D., Judge, M., Nye, V., Benzie, J., Antoniacomi, A., Coughlan, M., Morris, K. (2013). Moytirra: Discovery of the first known deep-sea hydrothermal vent field on the slow-spreading Mid-Atlantic Ridge north of the Azores. *Geochem. Geophys. Geosystems*, 14, 4170-4184. doi:10.1002/ggge.20243

White, D.A. (1993). Geologic risking guide for prospects and plays. *AAPG Bulletin*, 77, 2048–2061.

White, D.A. (1988). Oil and gas play maps in exploration and assessment: *AAPG Bulletin*, 72 (8), 944-949.

Wilcock, W. S. D., Hooft, E. E. E., Toomey, D. R., McGill, P. R., Barclay, A. H., Stakes, D. S., Ramirez, T. M. (2009). The role of magma injection in localizing black-smoker activity. *Nature Geoscience*, 2, 509-513.

Wilcock, W. S. D., & Delaney, J. R. (1996). Mid-ocean ridge sulfide deposits: Evidence for heat extraction from magma chambers or cracking fronts? *Earth Planet. Sci. Lett.*, 145, 49-64.

Wyborn, L. A. I., Heinrich, C. A., & Jaques, A. L. (1994). Australian Proterozoic mineral systems: essential ingredients and mappable criteria. *Australian Institute of Mining and Metallurgy Annual Conference, Melbourne, Proceedings*, 109-115.

Yang, J. (2002). Influence of normal faults and basement topography on ridge- flank hydrothermal fluid. *Geophysical Journal International*, 151, 1, 83-87.

Yeo, I. A., Clague, D. A., Martin, J. F., Paduan, J. B., & Caress, D. W. (2013). Pre-eruptive flow focussing in dikes feeding historical pillow Ridges on the Juan de Fuca and Gorda Ridges. *Geochemistry, Geophysics, Geosystems*, 14(9), 3586-3599. doi:10.1002/ggge.20210

Yeo, I. A., & Searle, R. C. (2013). High-resolution Remotely Operated Vehicle (ROV) mapping of a slow-spreading ridge: Mid-Atlantic Ridge 45°N: *Geochemistry, Geophysics, Geosystems*, 14, 1693-1702. doi: 10.1002/ggge.20082

Yeo, I. A., Searle, R. C., Achenbach, K. L., Le Bas, T. P. & Murton, B. J., 2012. Eruptive hummocks: Building blocks of the upper ocean crust. *Geol. Soc. Of Am.*, 40 (1), 91-94.

Zierenberg, R. A., Fouquet, Y., Miller, D. J., Bahr, J. M., Baker, P. A., Bjerkgard, T., Brunner, C. A., Duckworth, R. C., Gable, R., Gieskes, J., Goodfellow, W. D., Groschel-Becker, H. M., Guerin, G., Ishibashi, J., Iturrino, G., James, R. H., Lackschewitz, K. S., Marquez, L. L., Nehlig, P., Peter, P. M., Rigsby, C. A., Schultheiss, P., Shanks, W. C., III, Simoneit, B. R. T., Summit, M., Teagle, D. A.H., Urvat, M., & Zuffa, G. G. (1998). The deep structure of a sea-floor hydrothermal deposit. *Nature*, 392, 485-488.

Zierenberg, R. A., Schiffman, P., Jonasson, I. R., Tosdal, R., Pickthorn, W., & McClain, J. (1995). Alteration of basalt hyaloclastite at the off-axis Sea Cliff hydrothermal field, Gorda Ridge. *Chem. Geol.*, 126, 77-99.

Table 1. Mineral system model for seafloor sulfide deposits generated within neo-volcanic zones of mid-ocean ridges.

Critical process (assumption)	Geological signature (interpretation)	Proxies* (observation)
<p>(I) Heat source</p> <p>Magma intrusions (e.g., dikes and plutonics) during the spreading of oceanic crust.</p>	<ol style="list-style-type: none"> <li data-bbox="418 688 727 1459">Axial topographic highs (inflated ridge axis) built-up from volcanic products (e.g., eruptive fissures, smooth lava flows, flat-topped, mound- and crater-type volcanoes, volcanic hummocks and hummocky ridges; Smith and Cann 1990, 1999; Smith et al. 1995; Rubin et al. 2012; Yeo et al. 2012, 2013; Yeo and Searle 2013) that have morphologies varying from low relief to steep-edged mounds depending on the flow characteristics of the extruding melt (Lawson et al. 1996) and the spreading phase (Parson et al. 1993). <li data-bbox="735 688 1117 1459">Distinct ridge configuration: (i) symmetric ridge segments commonly suggest enhanced magmatism while (ii) an asymmetric system reveals tectonically-controlled extensions generally through a large-offset normal fault (detachment fault) accommodating a part of the plate separation along one of the ridge flanks (Tucholke et al. 2008). For the latter, faulting usually generates structures such as oceanic core complexes that can mine heat near a deep melt-rich zone (Dick et al., 2000) and carry gabbroic intrusions (Escartin et al., 2008) providing heat to off-axis hydrothermal convection cells (deMartin et al., 2007; Petersen et al., 2009). <li data-bbox="1125 688 1328 1459">Diverse dimensions of axial highs can be inferred from e.g., (i) the along-axis extents of neo-volcanic segments that can propagate or retreat from non-transform offsets, indicating major or minor magma supply respectively (Gràcia et al., 1997) and (ii) their aspect ratio (i.e., rift valley flank height/axial width; Murton and Rona, 2015). 	<ol style="list-style-type: none"> <li data-bbox="418 144 621 688">Extent of an axial-magma chamber (e.g., magnetotelluric, electro-magnetic and seismic surveying; e.g., Sinha et al., 1998; Carbotte et al., 2000; Singh et al., 2006) and melt distribution (seismic surveying; Kent et al., 2000). <li data-bbox="630 144 760 688">Magma budget evidenced from (i) the MgO content of axial basalts and (ii) negative residual gravity (Scheiter and Macdonald, 1993). <li data-bbox="768 144 865 688">Volume of erupted volcanics inferred from elevation data of axial highs (e.g., Smith et al., 1995).

(2) Pathways

- | | |
|--|---|
| <p>1. Zones of weakness characterized by increased tectonic activities as inferred from (i) axial and off-axis high-angle normal faults (Smith et al., 2008; Lavie et al., 1999), sometimes in the form of complex deformation zones where two linked co-linear faults join at depth (McAllister and Cann, 1996), (ii) detachment-like fault types, usually conducting to corrugated or non-corrugated core complexes during long-lived stretching phases (Reston and Ranero, 2011), and (iii) transfer zones bounding ridge segments, which accommodate large vertical throws (e.g., Dauteuil and Brun, 1996).</p> <p>2. Dilation zones and fracturing induced by subsidence (e.g., rift, graben- and caldera-like depressions; Rubin and Pollard, 1988; Baker et al., 1990; Pedersen et al., 2010), diking (Rubin and Pollard, 1988; Rubin, 1992) or tectonic stress release at e.g., cross-cutting faults (Curewitz and Karson, 1997), as observed locally for diverse hydrothermal vent systems (e.g., Karson and Rona, 1990; Murton et al., 1994; Cherkashov et al., 2008; Wheeler et al., 2013).</p> <p>3. High basement relief causing lateral pressure gradients in the crust and driving lateral fluid flows through the permeable crust (Fisher et al., 1994; Bani-Hassan, 2012). This mechanism, combined with active faults, may serve as focalizing high-velocity fluid migration toward the distanced ridge flanks (Yang, 2002).</p> | <p>1. Hydrothermal cell structure inferred from e.g., low seismicity surveying (Tolstoy et al., 2008).</p> <p>2. Pressurized cracking above magma chamber inferred from e.g., seismic records of hypocenters generated by stress perturbations (Wilcock et al., 2009).</p> <p>3. Faulting and sedimentary units inferred from seismic surveying and multibeam data (e.g., Bruvold et al., 2009).</p> <p>4. Zones with increased faulting investigated through earthquake swarms (Sørensen et al., 2007; Schlindwein et al., 2015).</p> <p>5. Vented hydrothermal plumes inferred from e.g., “tow-yo” conductivity-temperature-depth investigations (e.g., Walker et al., 2004; Melchert et al., 2008) and chemical analysis of the water column for which high content of dissolved substances such as CH₄, CO₂, H₂, H₂S, Fe and Mn may be indicative of hydrothermal activity (German and Von Damm, 2004).</p> |
|--|---|

<p>(3) Trap</p> <p>Precipitation of metal-rich sulfide minerals due to physico-chemical changes of circulating hydrothermal fluids; the precipitation can be processed below a capping system or overburden materials limiting the discharge and dispersion of residual fluids.</p>	<p>1. Conductive cooling and subsurface mixing of hydrothermal fluids with cold seawater (e.g., the TAG vent field; Tivey et al., 1995, 1998; Mills et al., 1998; Mills and Tivey, 1999) inducing changes of temperatures, pressure, pH, salinity and redox state (Reed and Palandri, 2006).</p> <p>2. Biotically-mediated precipitation of metal sulfides from sulfate-reducing bacteria in anoxic environments (Dvorak et al., 1992; Ehrlich, 1999; Labrenz et al., 2000).</p> <p>3. A capping system, such as (i) the sulfide mound, often topped by ocherous Fe-oxide deposits (Fouquet et al., 1988, 1993; Hannington et al., 1998), which structurally restrict fluid dispersion and contained sulfide minerals to oxidize and dissolve, (ii) sediments and mass-wasted materials, which can interact with the ascending fluids and make the fluids depleted in metals within conditions where mixing and oxidation by seawater prevails to form e.g., interlayered pyrrhotite-rich massive sulfides and sulfide-cemented sediments (Koski et al., 1994), (iii) mound-like structures of clastic sulfide units mixed with hemipelagic and turbiditic sediments overlain by fine-grained Cu-Fe-sulfide assemblages (Davis et al., 1992), and (vi) a low-permeability structure such as silica-cemented breccias (e.g., Zierenberg et al., 1995; Langmuir et al., 1997; Lisitsyn et al., 1989; Delaney et al., 1992), or series of lava flows (e.g., Ondréas et al., 2009; Humphris et al., 2002) pooling the upwelling hydrothermal fluids and forcing fluids to flow laterally and precipitate Cu-rich sulfide minerals while cooling, as observed, e.g. at the Bent hill hydrothermal site (Zierenberg et al., 1998); at this site a deep copper zone appear to replace present turbidite sediments with predominantly pyrrhotites and isocubanites, both generally formed within minor oxidizing conditions (Koski et al., 1985; 1988).</p>	<p>1. Gravitational collapses and related mass wasting deduced from high-resolution multibeam data (Cannat et al., 2013).</p> <p>2. Shallow hydrothermal activity inferred from in-situ observations of diffuse venting (e.g., Zierenberg et al., 1995; Langmuir et al., 1997).</p> <p>3. Seafloor and subsurface morphology (e.g., high-resolution multibeam, backscatter, side-scan sonar and sub-bottom profiler surveying; Caress et al., 2008; Honscho et al., 2015)</p>
--	---	---

<p>(4) Reservoir</p>	<p>Rock enclosing economically valuable metals (e.g., Zn, Cu, Ag and Au, ±Pb), first accumulated as sulfide minerals within a subsurface porous and permeable substratum (igneous or sedimentary), and then, preserved from dissolution and oxidation.</p>	<ol style="list-style-type: none"> 1. Mound-shaped orebody (e.g., Hannington et al., 1998; Webber et al., 2015) or “forest-like” chimney accumulations (Firstova et al., 2016), usually with a stringer zone (Zierenberg et al., 1998; Hannington et al., 1998). 2. Buried orebodies below subsequent lavas and/or sediments, occurring as e.g., (i) disseminations, veinlets, layers or pods transgressing within the bedding of their enclosing rocks, which are generally characteristic of stratabound deposits (Canavan, 1973) or (ii) stockwork deposits emplaced into fractures and cracks of a thick sequence of pillow basalt and basalt breccia, such as those observed within the ophiolitic sequence of the Northern Apennine ophiolites (Ferrario & Garuti, 1980; Garuti and Zaccarini, 2005; Garuti et al., 2008; Garuti et al., 2009). The preservation of buried deposits is best achieved on average 0.5 ± 0.2 km beneath the volcanic surface, before the crustal construction is complete at the time deposits are being displaced (Hall and Yang, 1994). 	<ol style="list-style-type: none"> 1. Low resistivity of oxidized sulfide mineral inside orebodies as measured from the self-potential method (Kawada and Kasaya, 2017). 2. Demagnetized rocks of hydrothermal upflow zones deduced from magnetic surveying (Johnson et al., 1982; Tivey et al., 1993; Tivey and Johnson, 2002). 3. Seafloor and subseafloor ground morphology (e.g., high-resolution multibeam, backscatter, side-scan sonar and sub-bottom profiler surveying; Caress et al., 2008; Honsho et al., 2015). 4. Layered mineralization determined from in-situ drilling (e.g., Fouquet et al., 1998; Zierenberg et al., 1998; Hannington et al., 1998; Lipton, 2012). 5. Rock samples from dredging to provide evidence of rocks affected by hydrothermal activity (e.g., Pedersen et al., 2010).
-----------------------------	--	---	---

*Non-exhaustive lists of possible indirect observation methods for the critical process of interest.

Table 2. Probability criteria applied to the geological factors of the study area.

PROBABILITY CRITERIA	CONDITION	VALUE*
Heat source (permissive tract level)		
P ₁ – Position compared to heat source	Within AVR zone	0.9
	Not within AVR zone	0.5
Trap (camp level)		
P ₂ – Sediments and seafloor mounds	Sedimentary terrains (i.e., ≤15° slopes)	0.8
	Mound structures	0.8
	Undetermined	0.5
Pathways		
P ₃ – Topographic disruptions (with buffer distances)	25-m distance	0.9
	50-m distance	0.8
	75-m distance	0.7
	100-m distance	0.6
	Undetermined or beyond 125m	0.5
Reservoir		
P ₄ – Sedimentary or mound-type terrain	Identified	0.8
	Undetermined	0.5

*Example of probability values attributed to the geological factors. The probability for each criterium is 1.0 for proven prospects.

Table 3. Probabilities of prospects*.

Criteria	P-1	P-2	P-3	P-4	P-5	P-6	P-7	P-8	P-9	P-10
Trap and seal	1.0	0.80	0.80	0.80	0.80	0.80	0.80	0.80	0.80	0.80
Reservoir presence	1.0	0.50	0.50	0.80	0.50	0.60	0.80	0.50	0.50	0.80
Pathways	1.0	0.80	0.80	0.90	0.80	0.90	0.90	0.50	0.90	0.60
Heat source	1.0	1.0	1.0	1.0	1.0	1.0	1.0	1.0	1.0	1.0

Prospect probability	1.0	0.32	0.32	0.58	0.32	0.43	0.58	0.20	0.36	0.38
----------------------	-----	------	------	------	------	------	------	------	------	------

*The numbering of prospects is shown on Fig.3. Probabilities are based upon in-situ observation of seafloor structuration and the nomenclature from [Rose \(2001\)](#) (section 2.3).

Table 4. Metal tonnage of prospects.

Variable	P-1	P-2	P-3	P-4	P-5	P-6	P-7	P-8	P-9	P-10
Area (m2)	37,527	3,618	3,121	54,677	2,257	6,788	13,846	5,957	3,490	33,743
Ore volume* (kt)	1042.4	100.5	86.7	1518.8	62.7	188.5	384.6	165.4	96.9	937.3
Total metals** (kt)	15.1	1.46	1.26	21.9	0.90	2.73	5.54	2.39	1.41	13.5

* Ore volume calculated using the ratio 27.7 t/m2.

** Amount of metals including Cu, Zn, Au and Ag given the ore potential of prospects and the grade models provided by [Mosier et al. \(2009\)](#). The calculation is processed stochastically using GeoX.

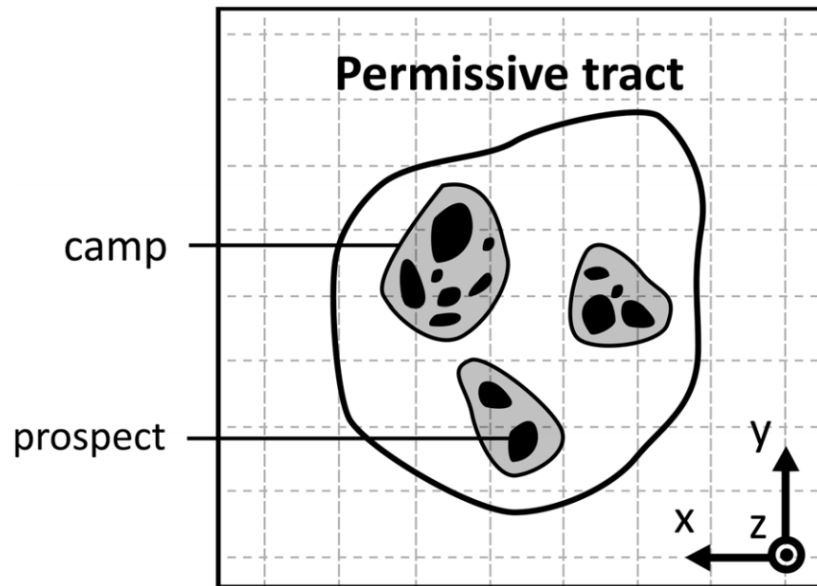


Fig.1 Schematic representation of a permissive tract, and respective camps and prospects, projected on a map. The view is from the top (Z is the depth below seawater).

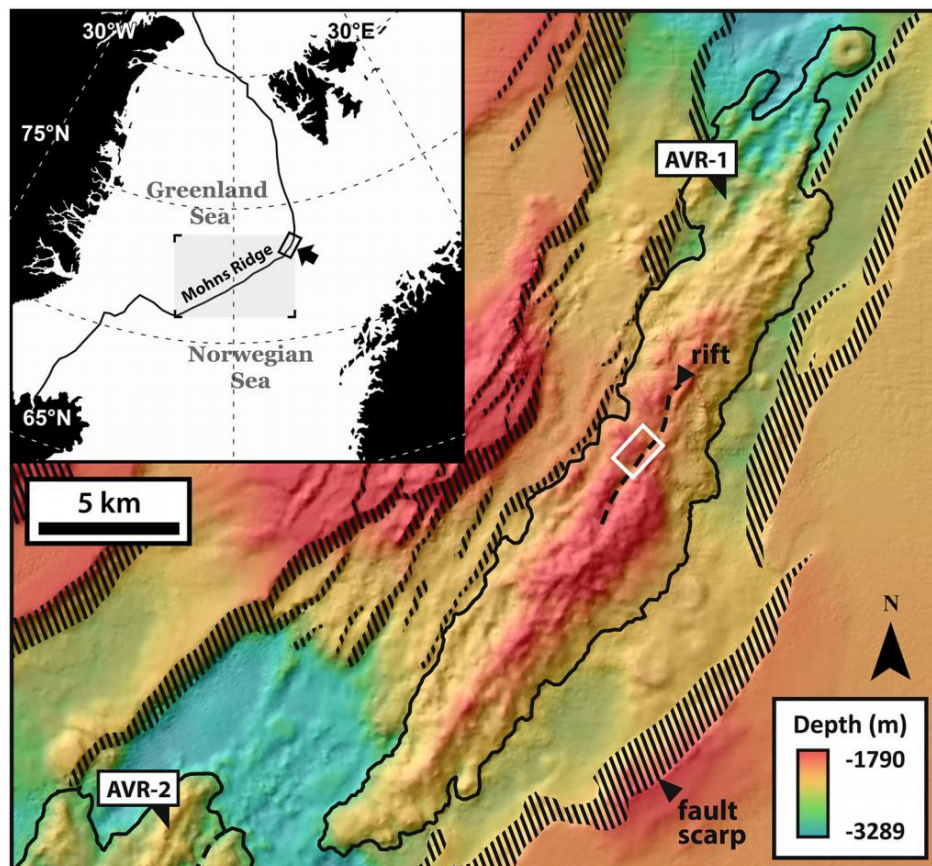


Fig.2 Location of the study area at the northernmost valley zone of the Mohns Ridge. Related axial volcanic ridge (AVR-1) is shown to have hummocky terrains and a rift zone where the high-resolution bathymetry of the Loki's Castle vent area (white rectangle) has been collected (see Fig.3).

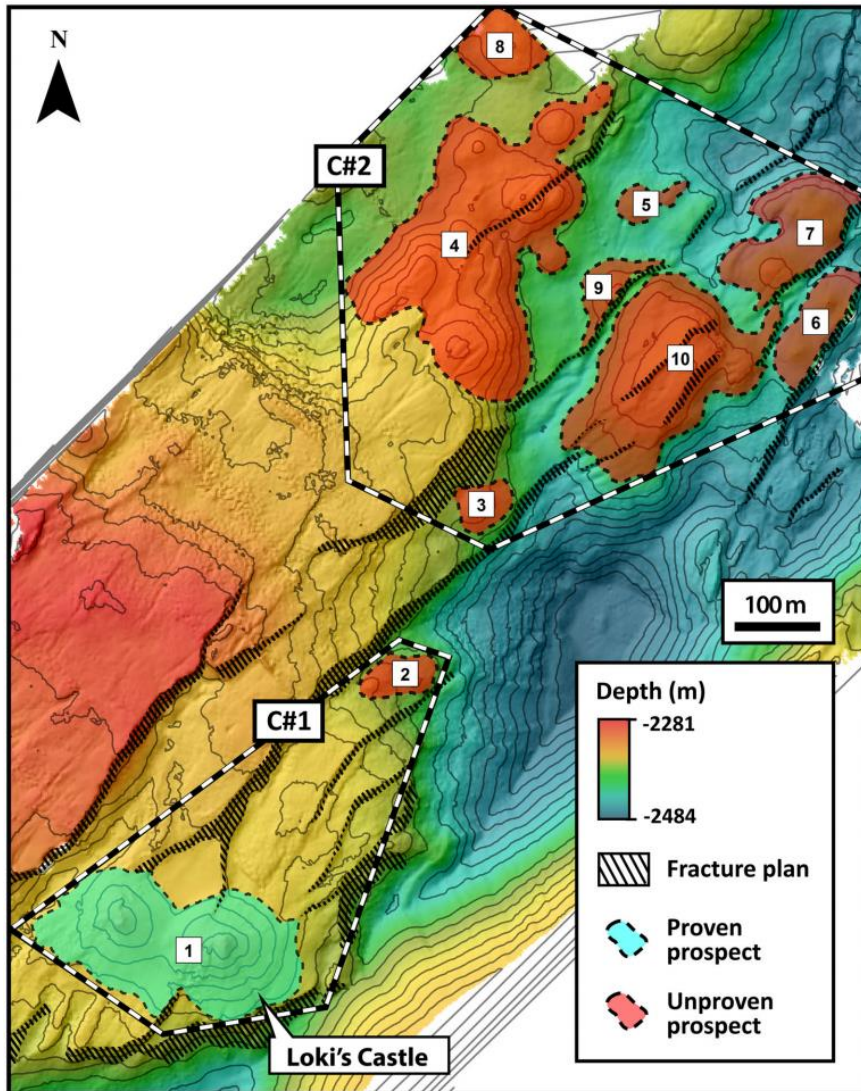


Fig.3 Bathymetric map of the study case presenting the Loki’s Castle sulfide mound (a proven prospect) and associated geological structures. Further north, other unproven prospects were delineated according to their identifiable mound-like structure; no direct observation data were collected during the MarMine cruise at those prospects. Prospects are aggregated into two different camps (C#1 and C#2) given their proximity. Contour interval is 8 m.

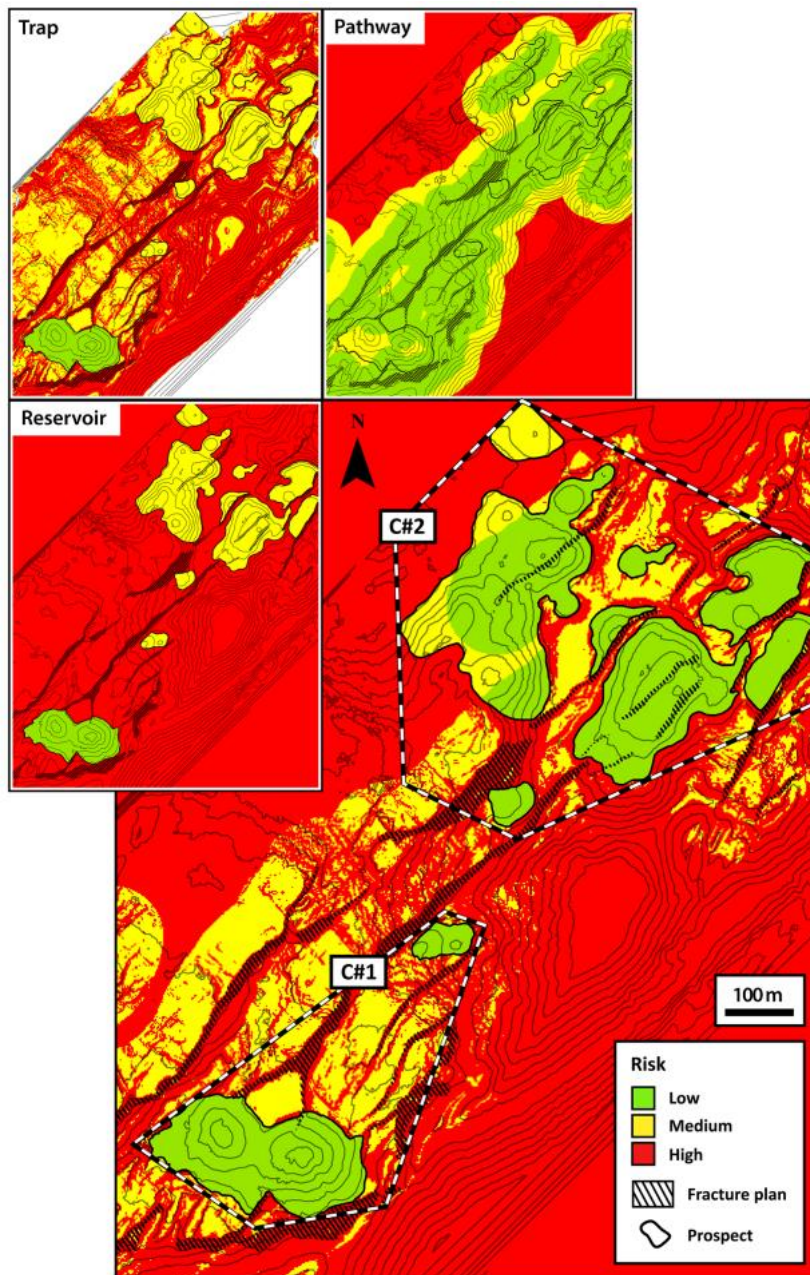


Fig.4 Risk map of the study area (bottom right) built on the combining of trap, reservoir and pathway risk values (top left). The risk values are either low (0 to 0.6), medium (0.6 to 0.75) or high (above 0.75) depending on the available data and related interpretations. Sedimentary traps are determined from slope values ($\leq 15^\circ$) given in-situ observations made during the MarMine cruise ([Ludvigsen et al., 2016](#)). Contour interval is 8 m.

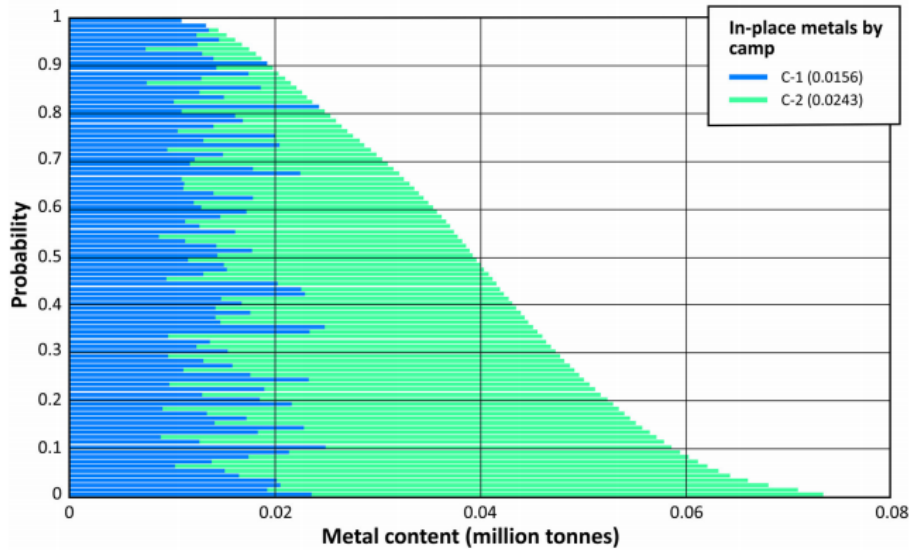
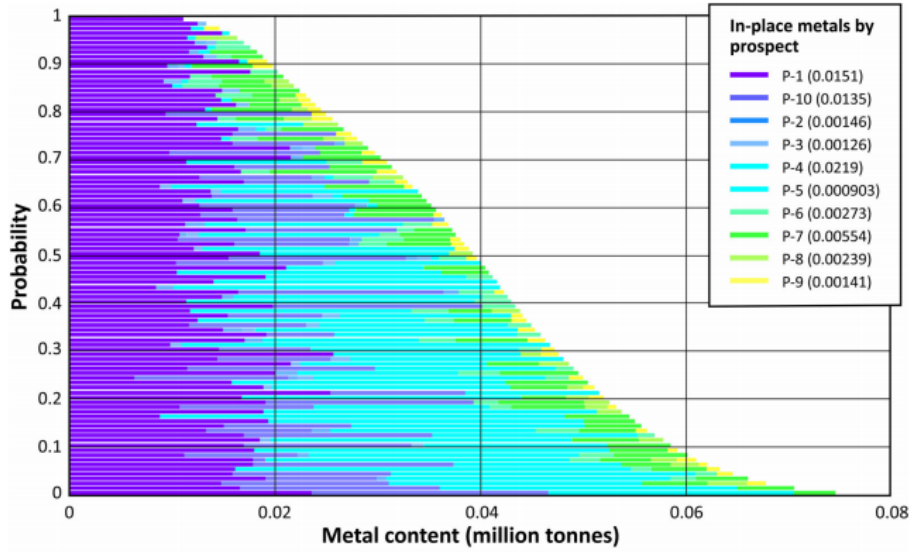


Fig.5 Resource diagrams calculated for each prospect (top) and camp (bottom). The number of sampling iteration is 10,000.

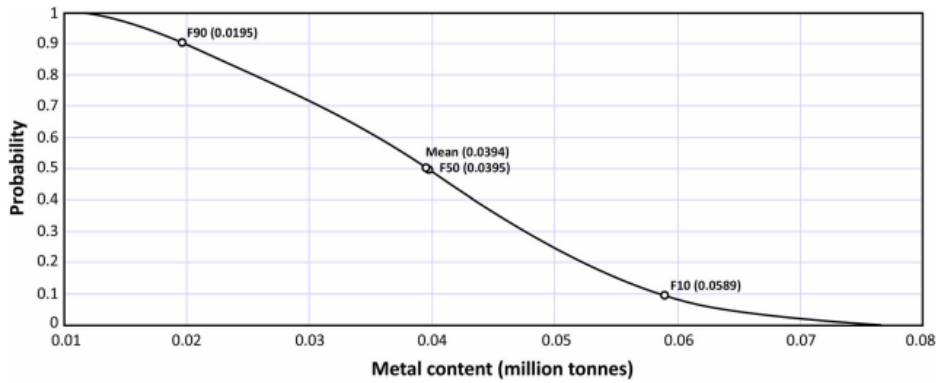


Fig.6 Cumulative distribution curve of total in-place metals estimated within the two camps. Percentiles (F10, F50 and F90) are indicated with respective resource volumes.